CSIRO Publishing

Publications of the Astronomical Society of Australia

VOLUME 18, 2001

An international journal of astronomy and astrophysics

For editorial enquiries and manuscripts, please contact:
The Editor, PASA,
ATNF, CSIRO,
PO Box 76,
Epping, NSW 1710, Australia
Telephone: +61 2 9372 4590
Fax: +61 2 9372 4310
Email: Michelle.Storey@atnf.csiro.au

For general enquiries and subscriptions, please contact:
CSIRO Publishing
PO Box 1139 (150 Oxford St)
Collingwood, Vic. 3066, Australia
Telephone: +61 3 9662 7666
Fax: +61 3 9662 7555
Email: pasa@publish.csiro.au

Published by CSIRO Publishing
for the Astronomical Society of Australia

www.publish.csiro.au/journals/pasa

Publ. Astron. Soc. Aust., 2001, 18, 76–83

First Results from the Combination of the AAO/UKST and Marseille Hα Surveys

D. Russeil[1,3,4] and Q. A. Parker[1,2]

[1]Anglo-Australian Observatory, Coonabarabran, NSW 2357, Australia
[2]Institute for Astronomy, Royal Observatory, Blackford Hill, Edinburgh EH9 3HJ, UK
[3]Observatoire de Marseille, 2 Place Leverrier, 13004 Marseille, France
[4]Observatory, University of Helsinki, PO Box 14, Helsinki, FIN-00014, Finland

Received 1999 December 1, accepted 2000 September 5

Abstract: We have combined the observational data of the AAO/UKST and Marseille Hα surveys to extract preliminary new results about ionised structures of our Galaxy. This includes the detection of a new large bubble located in the far part of the Carina arm.

Keywords: surveys: Hα — Galaxy: structure and kinematics — ISM: H II regions — ISM: individual (G297.506–0.765, G297.655–0.977, RCW48, G298.187–0.782, SNRG296.1–0.7)

1 Introduction

It is well established that Hα emission is the best tracer of star-forming complexes and hence of the spiral structure of galaxies (e.g. Hodge & Kennicut 1983; Considère & Athanassoula 1982, 1988). For external galaxies, the distribution of star-forming regions along the spiral arms is generally evident from direct imaging. In our Galaxy the spiral arms are strung out along the line of sight, which leads to the superposition and mixing of information from different spiral arm complexes, making it difficult to distinguish them. Hence, to study the detailed large scale structure of our Galaxy, we need to identify, discriminate and collect star-forming complexes and determine their distances. Distances are based on the correct identification of H II-region exciting stars within the complexes and/or on the determination of the systemic velocity. In practice, identification of H II-region exciting stars is difficult beyond 6 kpc from the Sun, due to interstellar absorption (e.g. Russeil 1998; Georgelin & Georgelin 1971; Forbes 1988). For the majority of H II regions, the only alternative is to obtain velocity information on the gaseous component. Although radio observations are useful in this regard, they do not enable resolution of the distance ambiguity problem for regions inside the Galactic solar orbit. Here Hα information is essential if we are to discriminate between the far and near distances proposed by the Galactic rotation model. Indeed, the detection of an Hα counterpart of a radio source or the detection of diffuse Hα emission at the same velocity as a star-forming complex will favour the choice of the near distance.

Determination of the spiral structure of our Galaxy is thus based on two important points: (i) the detection of Hα from H II regions, and (ii) accurate determination of their systemic velocities. The first point requires deep Hα imaging to detect faint H II regions from different spiral arms. The second point requires H II region velocities (including information on internal motions and close environment) and a large field of view to permit detection and grouping of sources with velocity departures from circular rotation and large-scale distribution on the plane of the sky. Observed velocity departures can be caused by energetic processes evolving in the Galactic disk, such as stellar winds from massive stars, supernovae explosions and impacts of high-velocity clouds on the Galactic disk. All these processes are sources of compression and acceleration of interstellar matter which can trigger star formation. Objects formed under these conditions may retain components of these accelerations (e.g. Rizzo & Arnal 1998), which then contribute to velocity departures from the Galactic rotation model. Bubbles, shells and cavities in the interstellar medium (ISM) observable at different wavelengths are the remnants of such process-induced star formation. It is important to identify these large structures and the H II regions they triggered for the best estimation of their systemic velocities.

In this paper we describe some initial combined results from two very different but highly complementary Galactic Plane (GP) Hα surveys which can help address these issues. These are the AAO/UKST and Marseille Hα surveys. In Section 2 we summarise the characteristics of the two surveys and in Section 3 present some preliminary results which illustrate the important additional insights that the combination of the two surveys offer for the study of Galactic structure.

2 The Data: The AAO/UKST and Marseille Hα Surveys

The main characteristics of the AAO/UKST and Marseille Hα surveys are summarised in Table 1 and described briefly below.

2.1 The AAO/UKST Hα Survey

The AAO is undertaking a photographic Hα survey of the southern GP and Magellanic Clouds, using the 1·8 m/1·2 m UK Schmidt Telescope (UKST). A monolithic 1% Hα interference filter with a 5° diameter circular

 10.1071/AS01001 1323-3580/01/010076$05.00

Table 1. The main characteristics of the two Hα surveys

	UKST	MHS
Telescope diameter (cm)	120/180	36
Field size (degree)	5·5	0·66
Filter FWHM (Å)	70	10
Central wavelength (Å)	6590	6562·78
Detector	Tech Pan film	IPCS+FP‡
Velocity information	none	All over the field FSR*: 115 km s^{-1} $\Delta v^{\star}$: 5 km s^{-1}
Typical resolution (arcsec)	∼2	>9
Approximate sensitivity	5 R†	<1 R†
Observing time (hr)	3	2

‡ IPCS+FP: Image Photon Counting System + Fabry-Perot
* FSR is the free spectral range of the interferometer
⋆ Δv is the spectral resolution
† R ≡ rayleigh. At $\lambda(\mathrm{H}\alpha) = 6563$ Å,
$1\,\mathrm{R} = 2{\cdot}41 \times 10^{-7}$ erg cm^{-2} s^{-1} ster^{-1}.

field of view on a 6·5° square glass substrate is being used; this is believed to be the largest astronomical single-element, narrowband filter. Deep 3 hr exposures are taken on fine-grained Kodak Tech Pan film on 4° field centres (necessary to achieve contiguous coverage of the GP). Detailed descriptions of the filter and survey are given by Parker & Bland-Hawthorn (1998) and Parker & Phillipps (1998a,b). This survey combines wide area coverage, good (∼2 arcsec) spatial resolution and decent (∼5 rayleigh) sensitivity to optical gaseous emission. Hα emission structures can be simultaneously examined at very small (a few arcsec) and very large (several degree) scales. Many kinds of extended Galactic objects are detectable, including discrete H II regions, diffuse emission patches, planetary nebulae (Parker, Russeil & Hartley, in preparation), large- and small-scale filaments, bubbles, shells, dark zones, supernovae remnants (Walker, Zealey & Parker 1999), Herbig–Haro objects (Mader et al. 1999), etc. Although morphological analysis of such emission structures can help to reveal connections between them, velocity information is crucial to unambiguously establishing any true physical relationship. However, there is no velocity information in the UKST Hα survey, given the 70 Å FWHM of the filter (∼3200 km s^{-1}). This is where the Marseille Hα survey comes into its own.

2.2 *The Marseille Hα Survey*

The Marseille Hα survey (MHS) is based on a scanning Fabry-Perot interferometer (Amram et al. 1991; le Coarer et al. 1992). The instrument, based at ESO (La Silla), provides spectral information for each pixel in the image plane. This allows a kinematic view of Hα emission to be built up as a datacube. Such information is essential to distinguishing different emission components along the line of sight. The observed line profiles are a superposition of these different emission contributions and the night-sky lines (geocoronal Hα and OH lines). After decomposition and subtraction of the sky, individual nebular components can be determined. This allows unbiased velocity estimates to be made for the detected ionised gas in the field. Both the intensity and velocity variation of each resolved Hα emission component can be determined across each field. Unfortunately, the MHS coverage of the GP is not continuous, the field of view is modest (0·66°) and the resolution is relatively low (the pixel size itself is 9 arcsec). Only the areas richest in H II regions have so far been covered. Field selection was based on previous radio and photographic Hα survey data (Georgelin & Georgelin 1970; Haynes, Caswell & Simons 1978). More recent radio surveys (Wright et al. 1994; Griffith & Wright 1993; Griffith et al. 1995; Gregory, Scott & Douglas 1996) and the AAO/UKST Hα survey reveal many more interesting zones to select for further follow-up with the MHS instrument.

2.3 *Survey Detection Limits*

The detection limits of each survey depend on the different characteristic parameters of the instrumentation and the type of observation. The MHS provides Hα spectra and channel maps, while the AAO/UKST survey provides Hα intensity maps integrated along the line of sight.

The high-spatial-resolution AAO/UKST survey exhibits high contrast between emission regions and adjacent dark zones while also revealing fine detail in faint Hα emission structures. With the MHS, an emission is detected if an associated component in the line profile is observed. The narrower filter bandpass (10 Å) decreases contamination from parasitic night-sky lines and continuum emission. This allows detection and discrimination of diffuse and uniform Hα emissions (e.g. the warm ionised medium, WIM) as well as more discrete and extended objects. However, due to the limited 9 arcsec pixel size, fine structures (e.g. filaments) will be diluted or unresolved. Although such detailed structural information is lost, velocity information exists so that such faint structures can be detected as faint components in the observed Hα profiles at different velocities from those of other diffuse emissions met along the line of sight.

At present no absolute comparisons of the depths of the two surveys are available. The MHS has not yet been systematically flux-calibrated (an estimation of 0·2 R for the faintest diffuse emission detected from a circular 30′ area by MHS can be found in Marcelin et al. 1998) and the AAO/UKST survey has not yet been properly calibrated. Work is currently under way to address these issues. For the AAO/UKST survey, preliminary results (J. Precious, private communication) reveal limits of about 5·1 R for two different UKST Hα survey fields. For the purposes of this paper, we illustrate the detection power via simple qualitative comparison. For overlapping areas of coverage between the two surveys, we looked for common detections in the Caswell & Haynes (1987) radio source catalogue. This was done because an important step in the study of our Galaxy's structure concerns the optical detection of radio sources. The two surveys detected the same radio sources down to the limit of 0·7 Jy.

2.4 The Importance of Wide Area Coverage and High Resolution

The AAO/UKST Hα survey allows detection of features of very large angular size while also providing fine detail on arcsecond scales. Such large features include bubbles, cavities, arcs, filaments, loops, superbubbles, supershells and supergiant shells (e.g. Tenorio-Tagle & Bodenheimer 1988). Some of these induce the velocity departures of the triggered H II regions, identification of which is crucial to studies of Galactic structure. In parallel, H II regions which are apparently isolated or well detached on the plane of the sky can be grouped into complexes by taking their velocities into account.

The high resolution of the AAO/UKST survey permits the precise morphology of H II regions to be seen. This is vital information in determining the location of the exciting stars via orientation of the observed rims and dust 'elephant trunks' with respect to the H II region as a whole (Pottash 1965; Herbig 1974). More precise determinations of the extent of H II regions can also be made (for example RCW105; Rodgers, Campbell & Whiteoak 1960). This additional structural information can account for the different diffuse emission components and their spatial intensity variations observed in the lower-resolution MHS mosaics.

The importance of the combination of high resolution and large field of view coupled with velocity information is illustrated by the following examples.

3 Some Preliminary Results

3.1 Identification of a New Large Structure at $l = 298°$

The Galactic direction $l = 298°$ is known to point between two spiral arms, implying weaker interstellar absorption towards this region. In radio emission, 10 sources (assumed to be H II regions) are observed with positive velocities in this direction (Caswell & Haynes 1987). Based on the mean rotation curve of Brand & Blitz (1993), this implies that these H II regions are located outside the solar circle at about 9.5 kpc from the Sun, and hence are localised in the far part of the Carina arm.

The MHS has surveyed this region and detected seven of these sources and several emission patches at the same velocity (Russeil 1997). These H II regions, being quite remote, exhibit small projected angular sizes (typically < 4 arcmin). The MHS is unable to provide much two-dimensional structural information for most of them. However, in the equivalent AAO/UKST Hα survey material the detailed morphology of these regions can be clearly seen. For example, we can see (Figure 1) that the known H II region G297·655–0·977 at $12^h01^m30{\cdot}3^s$, $-63°05'04''$ (Caswell & Haynes 1987) and a similar but newly discovered Hα/H II region at $11^h59^m45^s$, $-62°22'07''$ exhibit sharp, bright edges from where a more diffuse emission extends. This suggests that they are both located on the edge of a parental molecular cloud located to their east. Such detail is completely lost in the equivalent MHS images. This is the first time that the precise morphology of these H II regions has been seen. In addition, the associated AAO/UKST survey image (field HA135h, exposure HA17941) reveals a large, faint, diffuse emission region (Figure 2) which traces a semicircular structure of about 2° diameter centred at $12^h09^m24^s$, $-62°35'$ (298·5–0·3). This coincides in its southwest limb with the H II regions G297·506–0·765 ($12^h00^m33{\cdot}5^s$, $-62°35'$), G297·655–0·977 ($12^h01^m30{\cdot}3^s$, $-63°05'04''$) (Caswell & Haynes 1987), the region at $11^h59^m45^s$, $-62°22'07''$ and several emission patches detected at the same positive velocity by the MHS. The MHS data yield a velocity of $28\,\mathrm{km\,s^{-1}}$ for G297·655–0·977 (Figure 3) and $26\,\mathrm{km\,s^{-1}}$ for G297·506–0·765, as well as a mean velocity

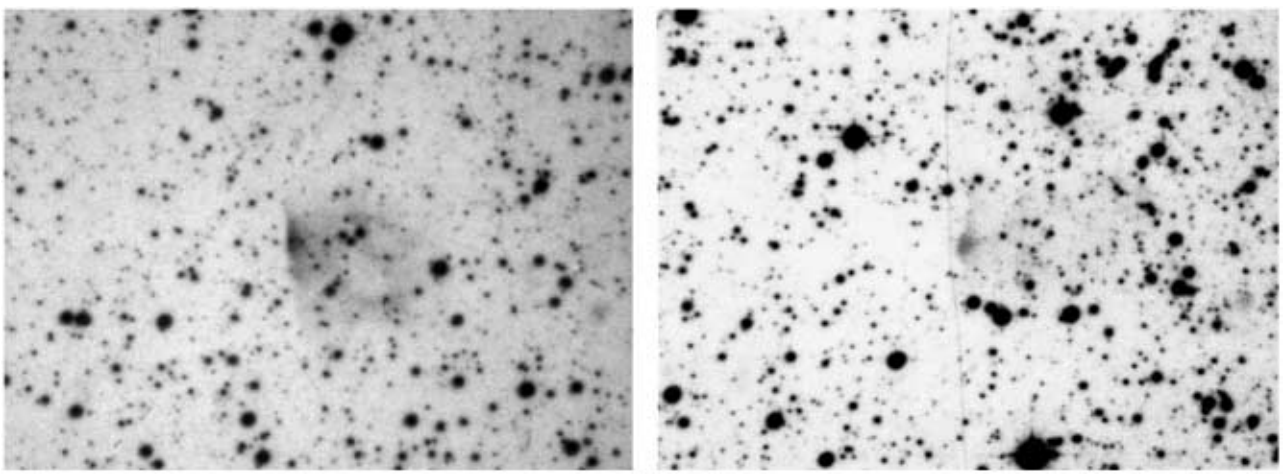

Figure 1 Hα images from the AAO/UKST survey of G297·655–0·977 ($12^h01^m30{\cdot}3^s$, $-63°05'04''$, B1950) (left) and the H II region at $11^h59^m45^s$, $-62°22'07''$, B1950 (right). The field of view of each image is $6' \times 4{\cdot}6'$, with north up and east to the left. The AAO/UKST image was obtained from a simple flatbed scan of a polaroid taken of these features from the original film (field HA135h, exposure HA17941). The detailed morphology of these regions suggests that they are at the edge of the same parental molecular cloud.

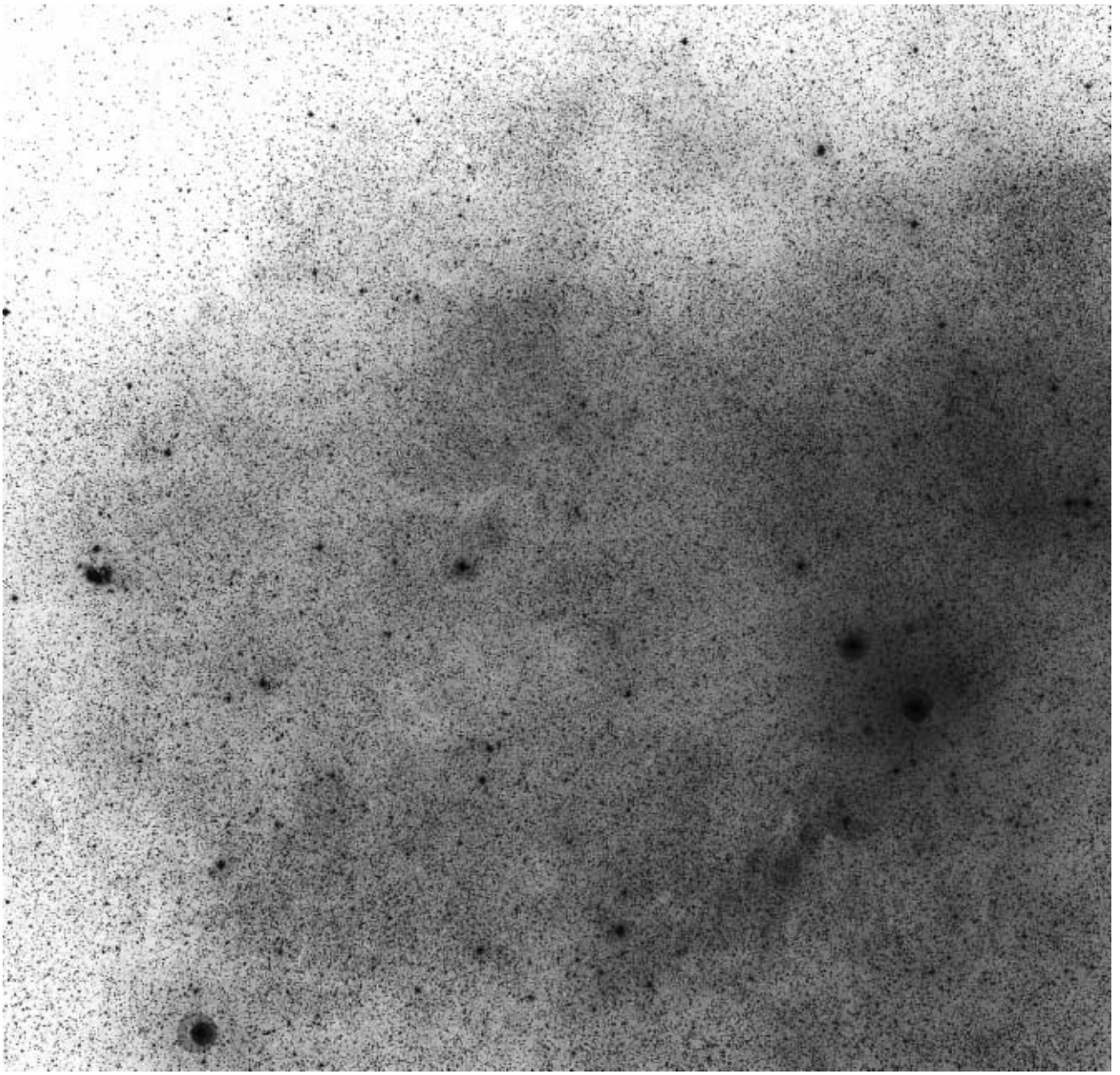

Figure 2(a) Hα image of the large semicircular structure centred at $12^{h}09^{m}24^{s}$, $-62°35'$, obtained from AAO/UKST survey field HA135h (exposure HA17941). The image was provided by direct photographic reproduction from the original film at the ROE photolabs. The field of view is about $3° \times 3{\cdot}3°$, with north up and east to the left.

of $28\,\mathrm{km\,s^{-1}}$ for several Hα patches, in good agreement with the radio data (Caswell & Haynes 1987).

These combined observations strongly suggest a link between these bright regions and the large semicircular structure with the giant molecular cloud n°26 (centre 298·8–0·2, $R_{\mathrm{eff}} = 124\,\mathrm{pc}$ with $d = 9{\cdot}5\,\mathrm{kpc}$, $V_{\mathrm{lsr}} = 25\,\mathrm{km\,s^{-1}}$) listed by Grabelsky et al. (1988). Moreover, the radius of the large structure ($R \sim 166\,\mathrm{pc}$ with $d = 9{\cdot}5\,\mathrm{kpc}$) is close to that of this molecular cloud n°26. Planned follow-up multi-spectral observations using the MHS instrument in other sections of this large circular structure will allow a more precise determination of this intriguing feature's nature and kinematics.

3.2 Morphology and Nature of Extended Emission Features

From MHS observations, diffuse emissions often appear as uniform layers across the field or as discrete patches of Hα emission at different velocities. The high resolution of the AAO/UKST survey allows clarification of the nature of these patches as filaments, sharp edges of bright clouds or more diffuse structures. Such structural information can help us to understand the different velocity components and intensity variations observed in these sources with the MHS. One good example is again given by objects detected in the AAO/UKST field HA135 h

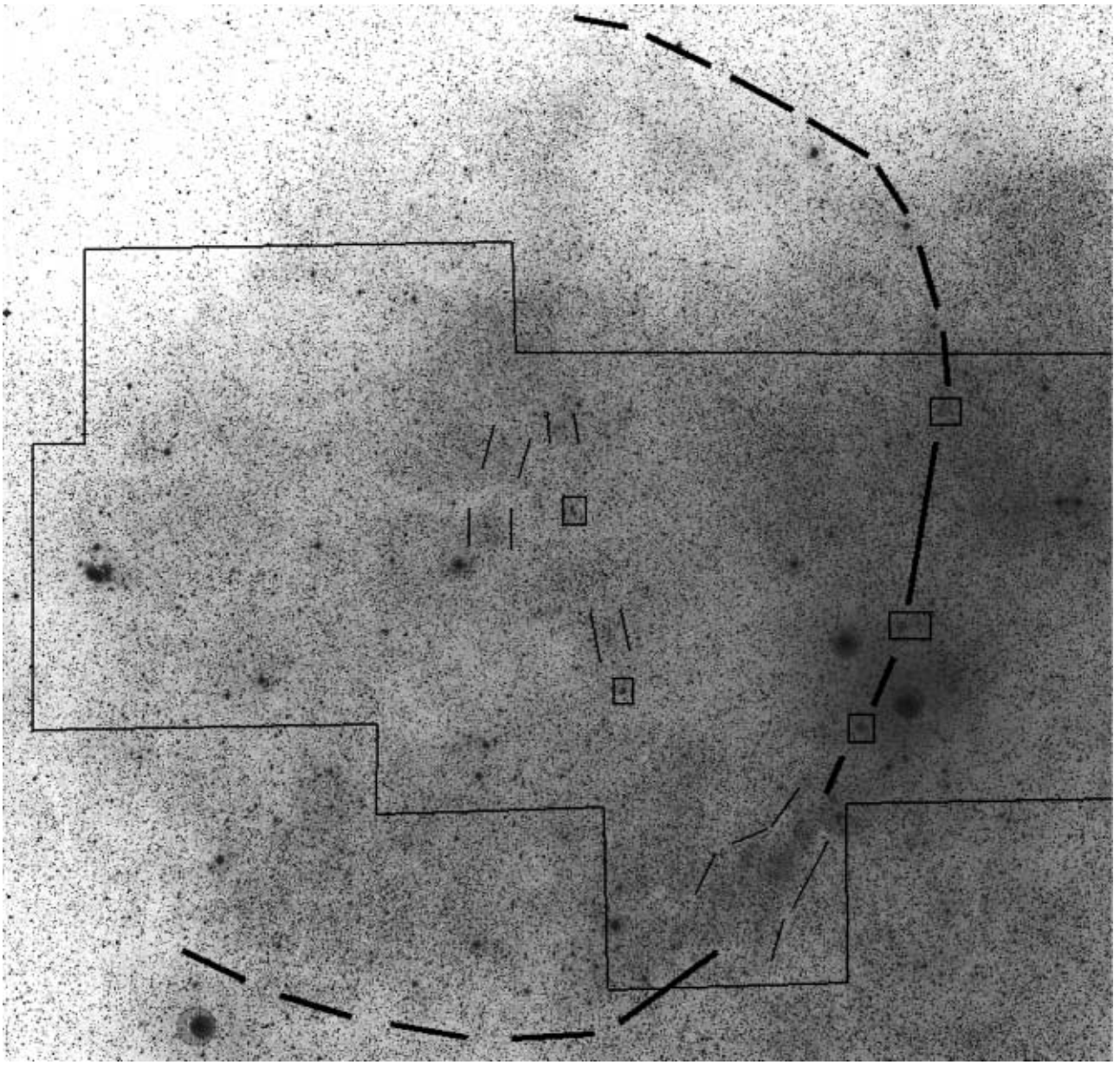

Figure 2(b) Same as Figure 2a but at normal contrast. The large structure is highlighted by the long-dashed lines. It seems to border the giant molecular cloud n°26 of Grabelsky et al. (1988). The framed area corresponds to the MHS-covered region. The small framed H II regions are (sorted by decreasing declination): the region at $11^h59^m45^s$, $-62°22'07''$; G298·22–0·331; G297·506–0·765; G298·187–0·782; G297·655–0·977. The areas within the quasi-parallel lines are zones where positive MHS velocity components were found. These zones, as well as the framed H II regions, are probably associated with the molecular cloud. Note that the other Hα reinforcements covered by the MHS have negative velocities. The prominent H II region on the left-hand side of the image is RCW64 ($V_{\rm lsr} = -40\,{\rm km\,s^{-1}}$).

(exposure HA17941) and the associated MHS Hα emission observed around 11^h50^m, $-62°15'$. The MHS data in this region reveal strong localised diffuse Hα emission extending across the entire 40 arcmin field of view (see Figure 1a in Russeil 1997) and with a mean velocity $V_{\rm lsr} = -34\,{\rm km\,s^{-1}}$. The extremely high intensity of this Hα emission is difficult to link with other fainter and smoother, diffuse emissions at negative velocity seen in the vicinity. Such emission can however be attributed to the large SNR G296·05–0·5 (Caswell & Barnes 1983). Many thin filaments around 11^h49^m, $-62°20'$ evident in the equivalent AAO/UKST Hα survey film (Figure 4) can clearly be linked to SNR G296·1–0·7 (Longmore, Clark & Murdin 1977; Whiteoak & Green 1996) which is a portion of SNR G296·05–0·5.

The detailed morphological study of Hα emission permitted by the high-resolution AAO/UKST survey images can also help us understand the physical connection of different emission features when kinematic information is not alone sufficient. Consider the case of RCW48 (Rodgers et al. 1960). This region is located towards the Galactic longitude 283°, which is known to be tangential to a spiral arm. Hence, in this special circumstance, features can have a large range in distance without exhibiting

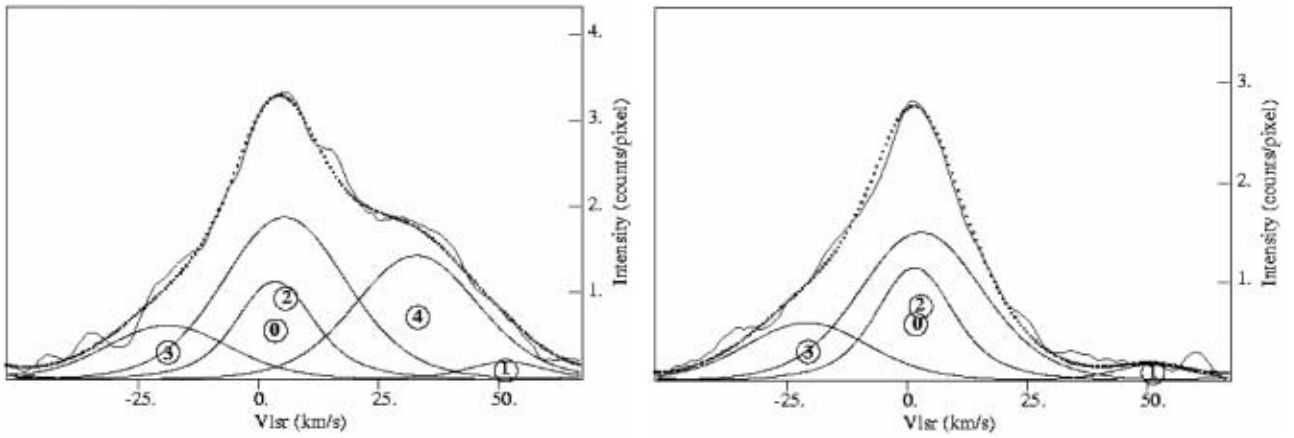

Figure 3 Hα profiles from the MHS, extracted for the area covered by G297·655–0·977 (left) and a nearby area (right). The components 0 and 1 are the night-sky lines while 2 and 3 are diffuse components at $V_{\rm lsr} = 5\,{\rm km\,s^{-1}}$ and $-18\,{\rm km\,s^{-1}}$ met along the line of sight. Component 4, which appears only in the left-hand profile, corresponds to the H II region. Its $V_{\rm lsr}$ is $28\,{\rm km\,s^{-1}}$.

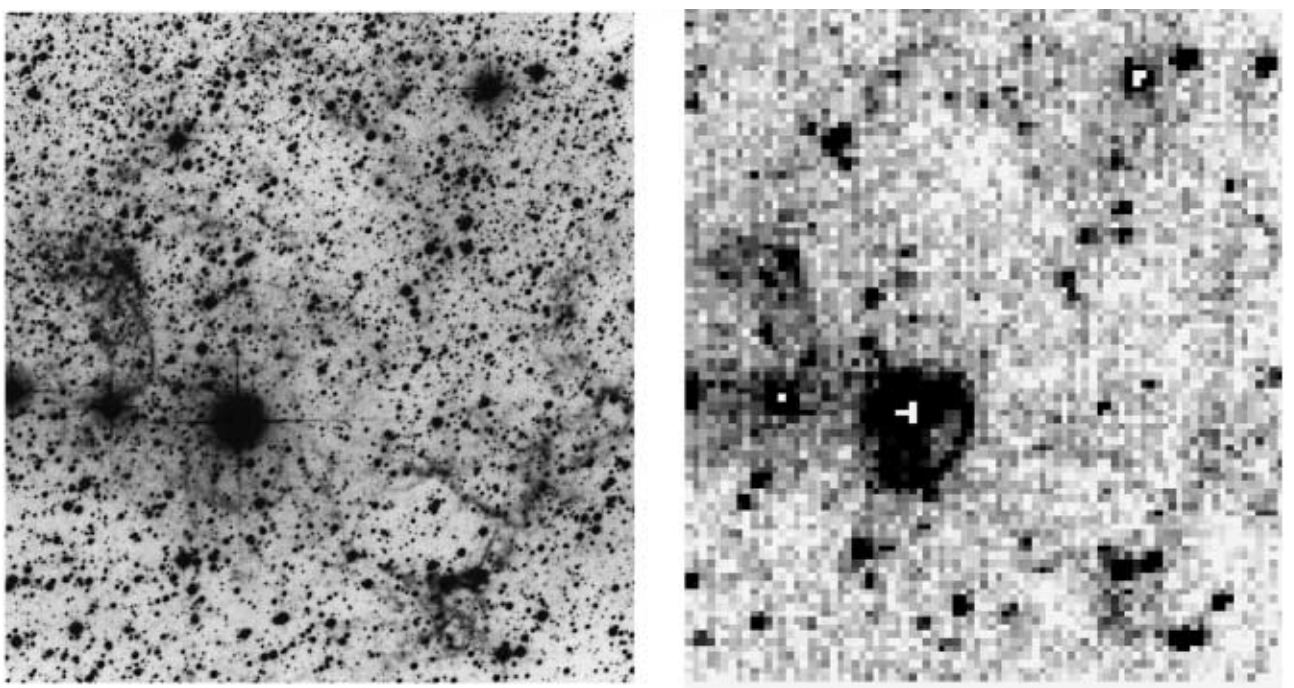

Figure 4 Hα images of the SNR G296·1–0·7 from the AAO/UKST survey (left) and MHS (right). The AAO/UKST image has been obtained in same way as Figure 2. The MHS image is from the combination of all λ-maps over the entire free spectral range of the Fabry-Perot interferometer (this corresponds to a monochromatic image of 10 Å bandwidth). The field of view of each image is about $12{\cdot}7' \times 13{\cdot}5'$, with north up and east to the left. The arc near the brightest star on the MHS image is an artefact. The fine detail in the AAO/UKST SNR image clarifies the nature of the Hα emission seen on the MHS image.

a corresponding difference in velocity. RCW48 is a large ionised region appearing as a collection of thin filaments and exhibiting a centre–edge velocity gradient (Deharveng & Maucherat 1974; Chu 1982). The MHS also detected this velocity gradient, with the outer part having a mean velocity of about $-8{\cdot}6\,{\rm km\,s^{-1}}$. There is also more extended, patchy, diffuse emission evident in the MHS data which exhibits a similar mean velocity of $-6\,{\rm km\,s^{-1}}$. Are these structures linked? On the AAO/UKST film, we can precisely delineate the structures belonging to RCW48 and clearly see a superposition with the more patchy background emission, with no obvious change of morphology or interaction evident between the two (Figure 5). This strongly suggests that this general patchy emission and that from RCW48 are not linked. We can conclude that they are at two different distances, tracing two different star-forming complexes.

4 Conclusion

The combination of the AAO/UKST and Marseille Hα surveys can provide a more complete description of southern Galactic Plane Hα emission than is possible with each

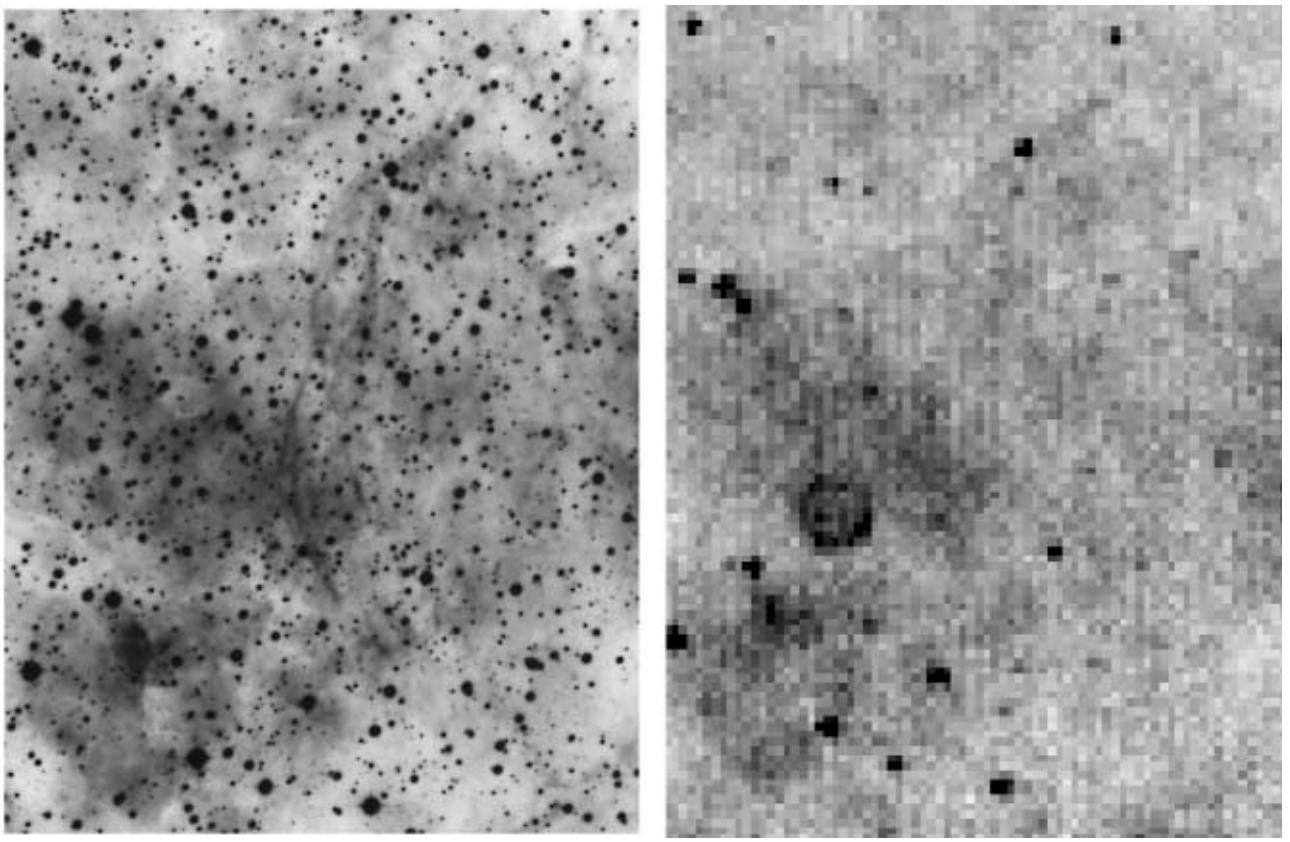

Figure 5 Hα images centred on $10^h17^m25^s$, $-57°45'$ (B1950) between RCW48 and RCW49 from the AAO/UKST survey (field HA222h, exposure HA17974, left) and the MHS (right). The images have been obtained in same way as Figure 4. The field of view of each image is about $11{\cdot}8' \times 15{\cdot}9'$, with north up and east to the left. The ring in the left-hand quadrant of the MHS image is another artefact. The AAO/UKST image clearly reveals the fine structure of the RCW48 filaments relative to the smoother, patchy background. Such features are beyond the MHS instrumental resolution and so are folded in to the general patchy emission.

survey separately. The important gains that come from combining the high resolution and large angular field maps of the AAO/UKST Hα survey with the velocity information revealed by the MHS has been illustrated in this paper by the new results obtained in the Galactic direction $l = 298°$.

The MHS not only provides velocity information but also allows the detection of the diffuse ionised component and more uniform gas layers, which are not readily detectable in the AAO/UKST Hα films. In parallel, the AAO/UKST survey allows detection of numerous new PNe candidates and faint compact H II regions over the entire southern GP, together with the study of their spatial distribution relative to more extended structures (SNR filaments, shells, loops, bubbles etc.). This should allow us to probe the physical environment of star formation and evolution.

The combined qualities of the AAO/UKST and MHS Hα surveys in delineating and unravelling Galactic structure, especially when compared with surveys at other wavelengths (e.g. CO, radio, MIR), should help us to solve several key problems in the study of our Galaxy. These include departures from circular rotation, the distance ambiguity problem and the limit and extent of star-forming complexes. We should also be able to estimate the input energy of the sources of ionisation, which can influence the kinematics, ionisation and composition of the ISM on medium scales.

Acknowledgments

D. Russeil was supported by a Lavoisier grant of the French Foreign Ministry, and acknowledges the hospitality of the AAO/UKST Observatory during her postdoctoral position. Much of this work was carried out when Q. A. Parker was on special leave from PPARC, working at the AAO. We thank the AAO/UKST for undertaking the Hα survey and the Hα survey consortium for providing the original scientific impetus. The authors thank the referees, Russell Cannon and an anonymous one, for useful suggestions and recommendations which have substantially improved the paper.

References

Amram, P., Boulesteix, J., Georgelin, Y. M., et al. 1991, The Messenger, 64, 44
Brand, J., & Blitz, L. 1993, A&A, 275, 67
Caswell, J. L., & Barnes, P. J. 1983, ApJ, 271, L55
Caswell, J. L., & Haynes, R. F. 1987, A&A, 171, 261
Chu, Y. H. 1982, ApJ, 254, 578
Considère, S., & Athanassoula, E. 1982, A&A, 111, 28
Considère, S., & Athanassoula, E. 1988, A&AS, 76, 365

Deharveng, L., & Maucherat, M. 1974, A&A, 34, 465
Forbes, D. 1988, A&AS, 77, 439
Georgelin, Y. P., & Georgelin, Y. M. 1970, A&A Supp. Ser., 3, 1
Grabelsky, D. A., Cohen, R. S., Bronfman, L., & Thaddeus, P. 1988, ApJ, 331, 181
Gregory, P. C., Scott, W. K., & Douglas, K. 1996, ApJS, 103, 427
Griffith, M. R., & Wright, A. E. 1993, AJ, 105, 1666
Griffith, M. R., Wright, A. E., Burke, E. F., & Ekers, R. D. 1995, ApJS, 97, 347
Haynes, R. F., Caswell, J. L., & Simons, L. W. J. 1978, Aust. J. Phys. Astrophys. Suppl., 45, 1
Herbig, G. H. 1974, PASP, 86, 604
Hodge, P. W., & Kennicut, R. C. 1983, AJ, 88, 296
le Coarer, E., Amram, P., Boulesteix, J., et al. 1992, A&A, 257, 389
Longmore, A. J., Clark, D. H., & Murdin, P. 1977, MNRAS, 181, 541
Mader, S., Zealey, W. S., Parker Q. A., & Masheder M. 1999, MNRAS, 310, 331
Marcelin, M., Amram, P., Bartlett, J. G., Valls-gabaud, D., & Blanchard, A. 1998, A&A, 338, 1
Parker, Q. A., & Bland-Hawthorn, J. 1998, PASA, 15, 33
Parker, Q. A., & Phillipps, S. 1998a, PASA, 15, 28
Parker, Q. A., & Phillipps, S. 1998b, A&G, 39, 10
Parker, Q. A., Russeil, D., & Hartley, M. 2001, in preparation
Pottash, S. R. 1965, Vistas in Astronomy, 6, 149
Rizzo, J. R., & Arnal, M. 1998, A&A, 332, 1025
Rodgers, A. W., Campbell, C. T., & Whiteoak, J. B. 1960, MNRAS, 121, 103
Russeil, D. 1997, A&A, 319, 788
Russeil, D. 1998, PhD thesis, Université de Provence
Tenorio-Tagle, G. 1979, A&A, 71, 59
Tenorio-Tagle, G., & Bodenheimer, P. 1988, ARA&A, 26, 145
Walker, A. R., Zealey, W. S., & Parker, Q. A. 1999, PASA, submitted
Whiteoak, J. B. Z., & Green, A. J. 1996, A&A, 118, 329
Wright, A. E., Gregory, P. C., Burke, B. F., & Ekers, R. D. 1994, ApJS, 91, 111